*Int. J. Electrochem. Sci.*, 7 **(2012)** 11219 - 11235

International Journal of
ELECTROCHEMICAL
SCIENCE
www.electrochemsci.org

# *Jathropha Curcas* and *Citrus Aurantium* Leaves Dye Extract for Use in Dye Sensitized Solar Cell with $TiO_2$ Films

*A. C. Nwanya*[1], *P.E. Ugwuoke*[1], *P. M. Ejikeme*[2], *O.U Oparaku*[1] *and F.I. Ezema*[3]

[1] National Centre for Energy Research and Development, University of Nigeria, Nsukka.
[2] Department of Pure and Industrial Chemistry, University of Nigeria, Nsukka
[3] Department of Physics and Astronomy, University of Nigeria, Nsukka
*E-mail: chinweasum@yahoo.com

*Received:* 22 August 2012 / *Accepted:* 28 September 2012 / *Published:* 1 November 2012

Study on dye-sensitized solar cells (DSSCs) with jathropha curcas and citrus aurantium leaf extracts as sensitizers is reported in this paper. DSSCs were assembled by using natural dyes extracted from jathropha curcas and citrus aurantium leaves as sensitizers and compared with that of ruthenium dye. $TiO_2$ films were prepared on FTO glass using the sol-gel process, the chemical bath deposition method and the slot coating of P-25 Degussa $TiO_2$ powder. The chemical, structural, morphology and optical properties of the$TiO_2$ were investigated using energy Dispersive Spectrum EDS, X-ray diffraction XRD, UV-Visible-Infrared spectroscopy and Scanning Electron Microscopy SEM. The slot coated $TiO_2$ with jathropha leaf dye extract showed the highest overall efficiency of 1.26% with open circuit voltage of 350mv, short circuit current of 65.5 μA and a fill factor of 0.55.

**Keywords:** Jathropha curcas, Citru aurantium, $TiO_2$, solar cell efficiency.

## 1. INTRODUCTION

Photovoltaic (PV) energy is known to be one of the cleanest energy sources with a very small carbon footprint. However, owing to the high cost of conventional solar cells, which are mainly based on Si, PV electricity is not competitive for large scale power production. Dye-sensitized solar cells (DSSCs) are attractive low cost PV cells and can be made by using a rather simple solution processing technique in a simple laboratory. Typically, DSSCs are composed of a dye-adsorbed nano-porous $TiO_2$ layer on a fluorine-doped tin-oxide (FTO) glass substrate, redox electrolytes and a counter electrode [1-6]. It has been shown that the efficiency of DSSC depends significantly the sensitizer used [7] and also on the properties of the nanostructured $TiO_2$ electrodes. Some of the properties of dye which determines the efficiency of the cell are; the absorption spectrum, the excited lifetime, dye-to-$TiO_2$

charge transfer and the anchorage of the dye to the surface of $TiO_2$. Commercially available dyes used mostly are ruthenium transition metal polypyridyl complexes such as N719 and N3 dyes, both of which have shown satisfactory photoelectric conversion efficiency. On the other hand, these dyes use some heavy metals which are difficult to synthesize, expensive, and are environmentally hazardous. Many kinds of natural dyes have been actively studied and tested as low-cost materials in order to replace the rare and expensive ruthenium compounds [7-10]. However, natural dyes usually gave poor photovoltaic response in DSSC but these dyes are very cheap and can be prepared easily, compared to ruthenium polypyridyl complexes. The nanosize $TiO_2$ colloids used for DSSC are sintered on a transparent conducting substrate. The sintering process forms electrical contact between the various colloids and between the colloids and the substrate [11]. The properties of the nano-structured $TiO_2$ electrodes also play a significant role in the overall efficiencies of the cell. For example, the surface area of the film determines the dye uptake, the pore size distribution affects the ion diffusion, the particle size distribution determines the optical properties and the electron percolation depends on the interconnection of the $TiO_2$ particles [12].

In this work $TiO_2$ electrode was prepared using the sol gel dip coating, chemical bath deposition and the slot coating methods. The prepared films were used for assembling samples of DSSCs using natural dyes extracted from jathropha curcas and citrus aurantium leaves. Jathropha curcas is grown widely in southern Nigeria primarily for fencing but recently as a source of bio-fuel. Citrus aurantium is grown mainly for the medicinal value of its fruit juice and for shade in most homes. It has been reported that jathropha leaf juice stains red and makes linen an indelible mark [13]. Jatropha seeds have been used in the production of bio fuels hence the motive to use its leaves is to ascertain whether the leaves are good candidate for natural dye for DSSC while the use of citrus aurantium was for comparative purposes. Because of the simple preparation technique, widely source, and cheap cost, natural dye as an alternative sensitizer for dye-sensitized solar cell is promising.

## 2. EXPERIMENTAL DETAILS

### *2.1 Extraction of natural dye and synthetic dye Preparation and Sensitization*

The dye sensitization of the electrodes was done using natural and in-organic dyes.

Fresh leaves of jathropha curcas ans citrus aurantium was obtained from the neighborhood of University of Nigeria, Nsukka. Boiling water was poured into a cup containing samples of the leaves until it covers the sample leaves and was left for about 1minute. The leaves were removed from the water and dried with paper towel. Boiling water kills the cells and destroys the enzymes which can promote chlorophyll degradation. It also breaks chloroplasts which makes chlorophyll extraction easier. The petioles and central veins were removed from the leaves because these parts of leaf do not contain a lot of pigments. The leaves were cut into small pieces and spread evenly on a foil and put in the oven for 20 minutes at $40^0$C. The dry leaves pieces were ground and the powder was put in a test tube with tight lid and a few milliliters of ethanol were added. The lid is closed and shaken. This was left for 24hrs in a dark cupboard and then is centrifuged. The supernatant was now poured into another

test tube and the lid was opened to concentrate the dye. The remaining plant pigment was now stored in a dark cupboard ready for use.

Inorganic dye used is ruthenium red dye R2751 $[(NH_3)_5RuORu(NH_3)_4ORu(NH_3)5]Cl_5$ obtained from Sigma-Aldrich company Germany. 3x $10^{-4}$ M solution of the synthetic dye was prepared by dissolving 10mg of the dry ruthenium dye powder in 25ml of methanol and stirring until no traces of solid dye are visible. The result was a dark purple solution which was stored in a non transparent bottle.

Three methods were used to deposit the $TiO_2$ electrode and they are:

### *2.1. Slot Coating Method using commercially available Titanium (IV) Powder.*

The colloidal $TiO_2$ paste was prepared using $TiO_2$ powder P25 Degussa based on the procedure described by Greg and Gratzel [11]. 6g of the aggregated powder was ground in a mortar and while grinding, 10ml of very dilute acetic acid with PH 3-4 in deionized water was added in drops of 1ml to prevent re-aggregation of the particles. After a colloidal suspension is obtained, few drops of Triton X-100 surfactant were added. Adhesive tape is applied on the conductive side of the fluorine doped tin oxide substrate FTO that has been cleaned to mask a strip of about 1mm on each side. Few drops of the $TiO_2$ suspension was applied on one edge of the substrate near the tape and a clean glass rod was used to slide the paste uniformly on the FTO. After the deposition the tape was carefully removed and the plate was allowed to dry for a few minutes at room temperature. This was then sintered at $400^0$C in an oven for 45minutes.

### *2.2. Chemical Bath Deposition Method*

5ml of 1M NaOH solution was put in a beaker containing 5ml of deionised water. 3ml of $TiCl_3$ (analytical grade) was gradually added to the solution while being stirred on a magnetic stirrer. After the addition of the $TiCl_3$ the entire solution was further stirred for about ten minutes. The FTO which has being cleaned as previously discussed is now immersed fully into the solution. The film is allowed to deposit on the substrate for 24 hours at room temperature. After which the substrate is brought out rinsed with deionised water and sintered at $400^0$C for 1 hour. The chemical reactions are as shown below:

$$Ti^{3+} + 3OH^- \longrightarrow Ti(OH)_3 \quad (1)$$

$$Ti(OH)_3 + OH^- \longrightarrow TiO_2 + 2H_2O \quad (2)$$

It was noticed that longer stay of the substrate in the solution gave a thicker deposition. Also the pH of the resultant solution is found to play vital role during film deposition hence the pH was maintained at 3.5 with the drop wise addition of NaOH solution at room temperature.

*2.3 Sol-Gel method*

1M NaOH was dissolved in 50ml of ethanol solution to which of 5ml of acetic acid has been added. The mixture was stirred vigorously on a magnetic stirrer at $65^0$C for 3hrs. 7ml of $TiCl_3$ was added dropwise to the solution while the stirring is on. It was observed that the each drop of $TiCl_3$ changes the sol to ash colour and then to white with continued stirring. Previously cleaned and taped FTO glass as described above is dipped into the solution. A gel film was formed on the FTO. This was left for a few minutes in the open air to dry and then sintered at a temperature of $100^0$C for 30mins. This was brought out and rinsed with deionised water and annealed again for 1hour at $400^0$C. The concentration ratio of $TiCl_3$ and acetic acid was altered to see the effects on the deposited film. The stirring time was also changed but the sol manufactured due to the method described above was used to produce coating on the substrate. The flow chart for the processes is as shown in figure 1.

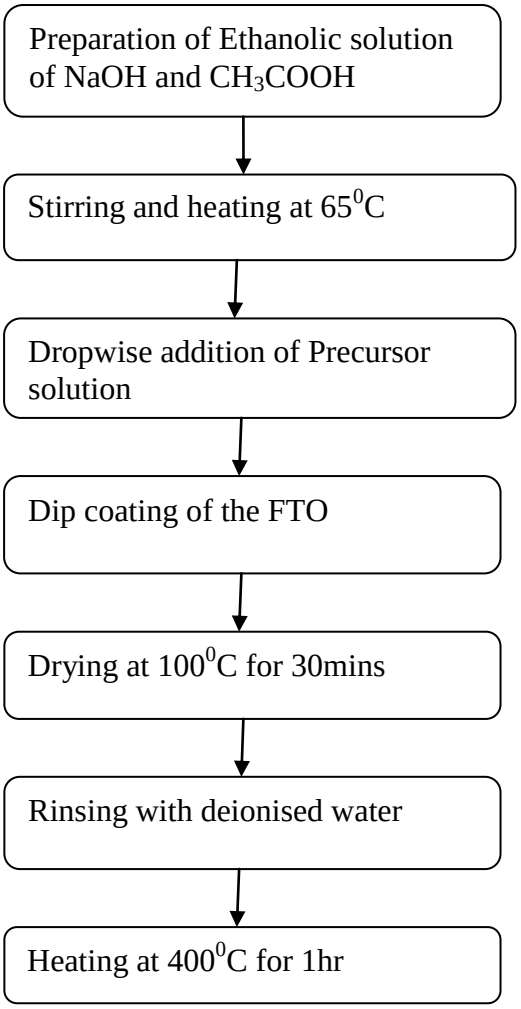


**Figure 1.** Flow chart for preparing titanium dioxide sol gel on FTO

*2.4 Electrolytes*

0.5M Potassium iodide KI was mixed with 0.05M iodine $I_2$ in acetonitrile. This was done by putting 0.127g of $I_2$ and 0.83g of KI in 10ml of acetonitrile. The mixture was stirred until all the solid has dissolved. The solution was stored in a dropper bottle for further use.

*2.5 Counter Electrode*

The counter electrode used is FTO coated with carbon. The conductive side of the FTO was cleaned as previously described and then coated with graphite. This was heated for a few minutes at $300^0$C in the oven. This was done so that the carbon will spread evenly on the FTO.

*2.6 Assembling the Cell*

The staining of the above prepared $TiO_2$ electrodes was done by heating the electrodes again to about a temperature of about $60^0$C in the oven and immersed immediately into the already prepared dye solution. The stained $TiO_2$ electrodes and the graphite coated counter electrode were assembled by placing the electrodes a little offset opposite to each other to expose contact areas for alligator clips and by pressing them together with binder clips. Few drops of the electrolyte were added to edge of the plate and by capillary action it travels between the two plates. Any excess electrolyte was removed from the edges of the cell with a paper towel.

## 3. RESULTS AND DISCUSSION

The results are discussed below:

*3.1 Energy-dispersive X-ray spectroscopy (EDS)*

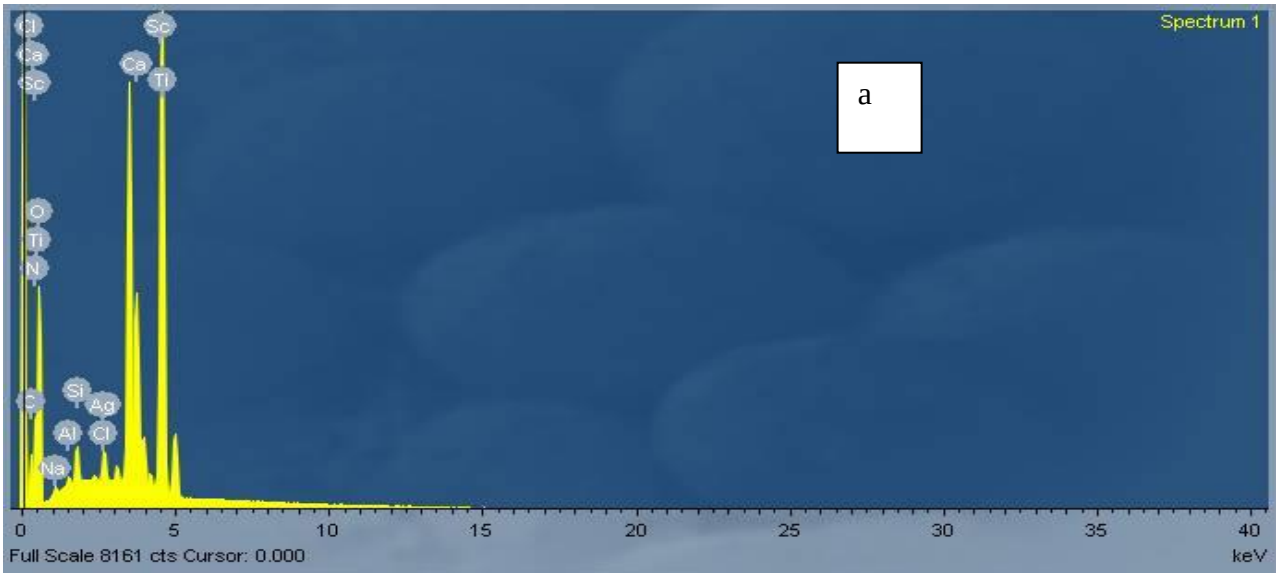

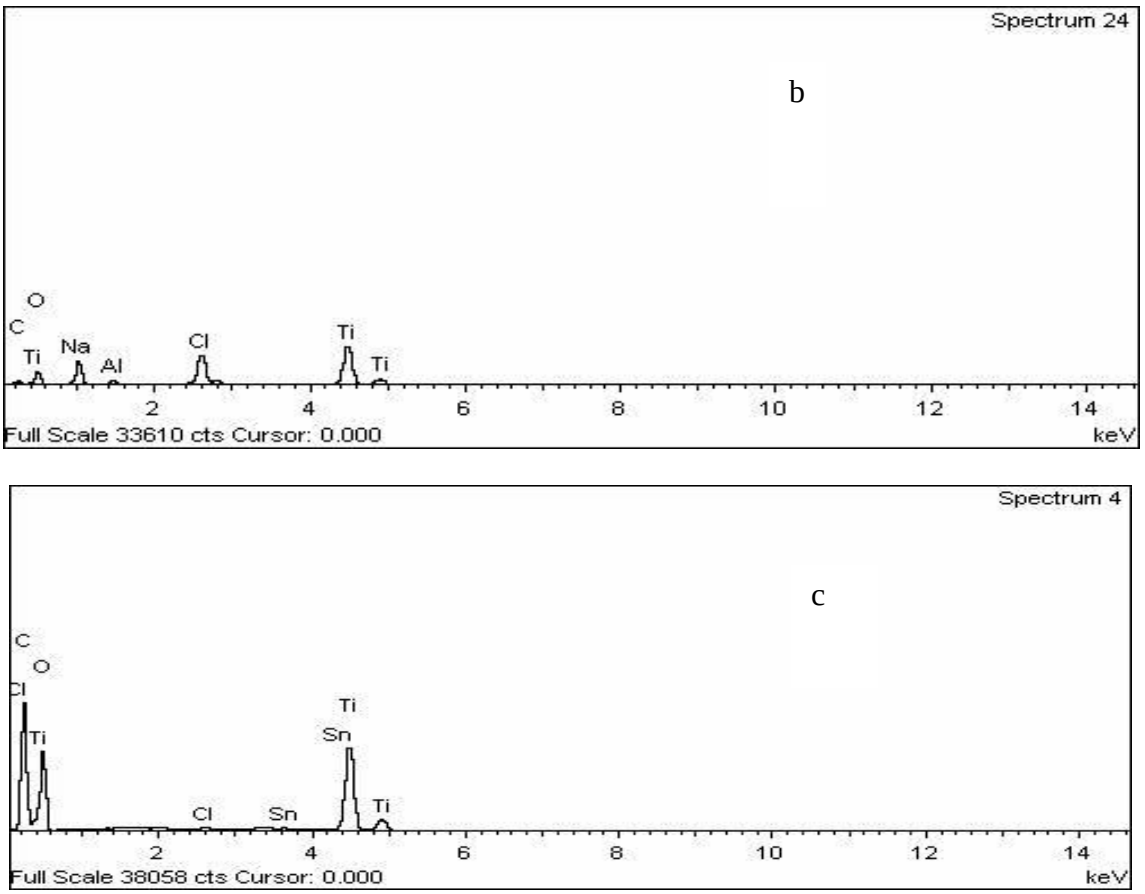


**Figure 2.** EDS spectrum of (a) CBD deposited $TiO_2$ (b) sol gel deposited $TiO_2$ (c) slot coated $TiO_2$

The chemical compositions of the deposited $TiO_2$ were determined by X-Ray Energy Dispersion spectroscopy (EDS) with accelerating voltage of 20kV. Figure 2 (a-c) shows the EDS data of CBD, sol gel and slot coated deposited $TiO_2$. The CBD spectrum shows the peaks of Ti and O. The presence of chlorine emanates from the precursor used and is typical for chloride type of precursors [14], while the other elements seen are due to the FTO glass used. Table 1 show the percentage weight and atomic percent of the chemical composition of the deposited film from sol gel and slot coated $TiO_2$. From the table, it is seen that carbon constituted about 12.15% in the sol gel deposited film while the atomic ratio of Oxygen to Titanium is 2.12: which is nearly that of $TiO_2$, with the difference remaining within the range of experimental error. The atomic percent of chlorine is 6.72 which is within the 3.3-7.5 range typical for chloride precursors [14, 15]**.** The chemical composition of the slot coated $TiO_2$ show a high percentage of carbon. This could be due to the surfactant Triton X 100 added. The ratio of oxygen to titanium is 3.01. Though this ratio is higher than the $TiO_2$ stoichiometric value, it still suggests a predominant presence of titanium dioxide. All the EDS spectra show the characteristic x-ray energy level of titanium ($K_\alpha$=4.510KeV and $K_\beta$=4.931KeV) and oxygen ($K_\alpha$ = 0.523KeV) [16].

**Table 1.** Elemental Composition of the deposited $TiO_2$

| Sol gel | | | Slot coating | | | | | |
|---|---|---|---|---|---|---|---|---|
| Element | Weight % | Atomic % | Element | Weight % | Atomic % | Element | Weight % | Atomic % |
| C | 12.57 | 12.15 | C | 36.53 | 38.31 | C | 8.95 | 9.15 |
| O | 35.55 | 47.04 | O | 46.54 | 46.20 | O | 36.28 | 48.16 |
| Na | 11.96 | 11.02 | Sn | 0.69 | 0.09 | Na | 10.66 | 9.92 |
| Al | 1.17 | 0.92 | Cl | 0.09 | 0.04 | Al | 1.04 | 1.89 |
| Cl | 11.25 | 6.72 | Ti | 16.15 | 15.35 | Cl | 13.52 | 6.75 |
| Ti | 27.50 | 22.15 | Total | 100.0 | | Ti | 29.58 | 24.15 |
| Total | 100.0 | | | | | Total | | |

*3.2 X-ray Diffraction (XRD)*

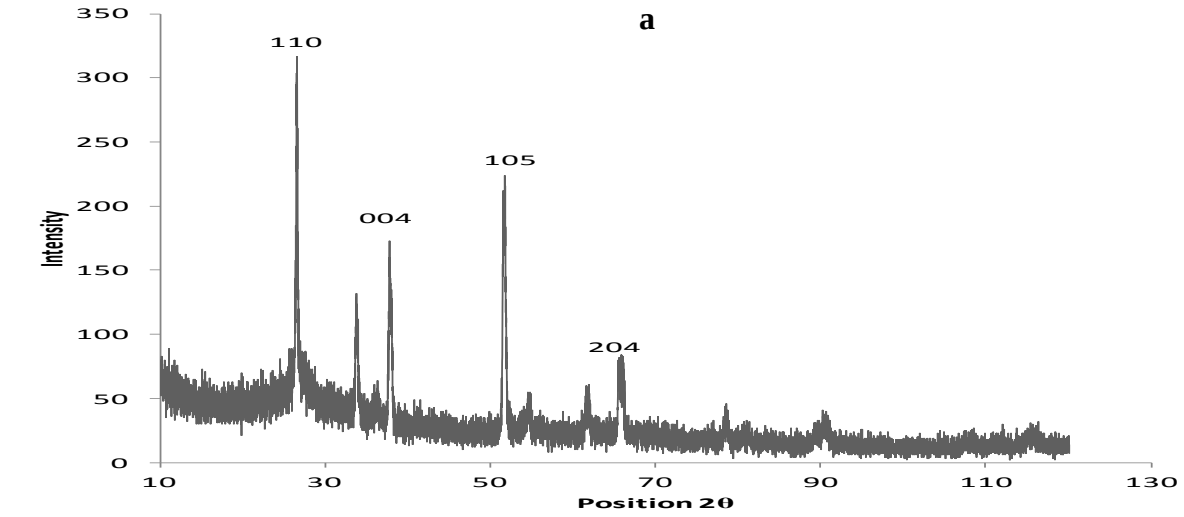


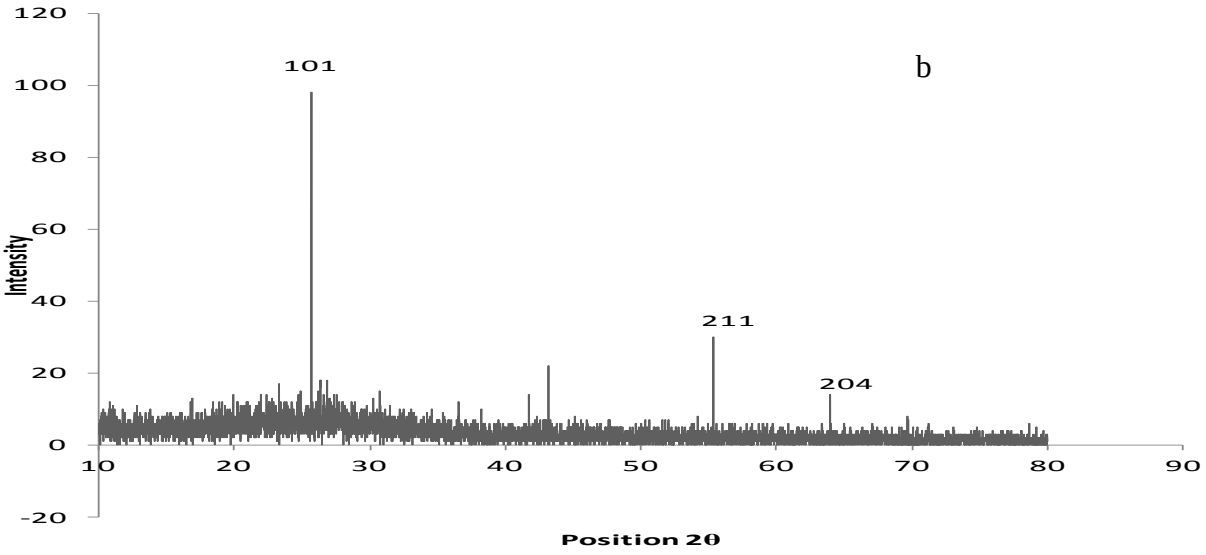

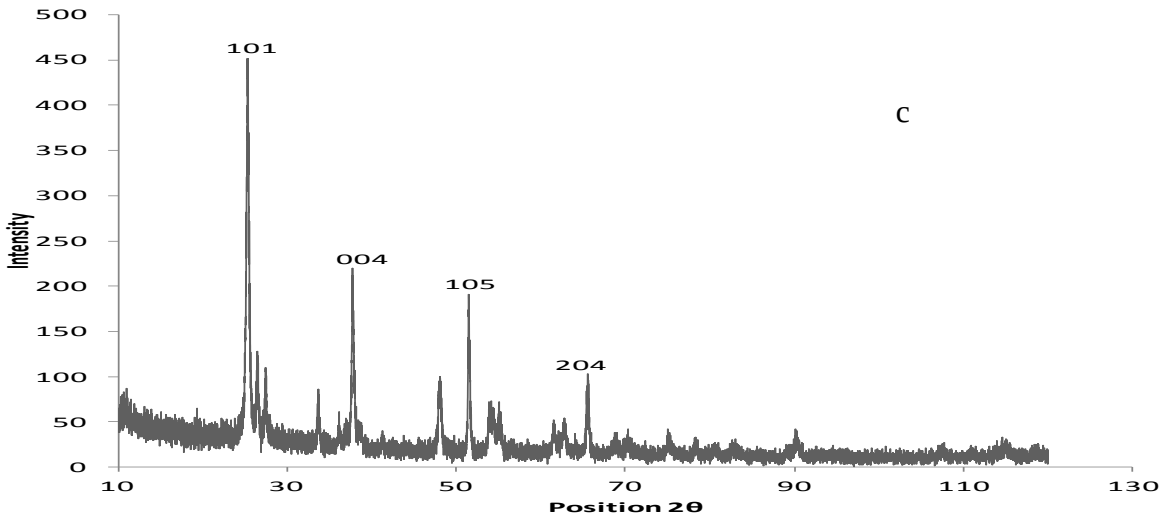


**Figure 3.** XRD pattern of (a) CBD deposited $TiO_2$ (b) sol gel deposited $TiO_2$ (c) slot coated $TiO_2$

The crystal structure and the phases present in the $TiO_2$ film were determined using XRD. The crystal grain size was estimated using Schererr equation:

$$D = \frac{K\lambda}{\beta \cos\theta} \qquad 3$$

Where K is a dimensionless constant often called the shape factor with a value of 0.9, λ is the wavelength of the x-ray radiation, β is the full width at half maximum (FWHM) of the diffraction peak and 2θ is the diffraction angle in degrees. Figure 3 (a-c) shows the X-ray diffraction patterns of the $TiO_2$ deposited by the three methods. The diffraction intensity was measured at $0.5^0$ incidence angle in the 2θ range between $10^0$ and $120^0$ with a step size of $0.01^0$. The CBD spectrum shows a mixture of rutile and anatase phases. Two sharp diffraction peaks of the anatase phase (004 and 204) corresponding to 2θ = 37.7, and 65.5 respectively, and two sharp peaks of rutile phase (110 and 105) corresponding to 2θ =26.5 and 52.5 respectively, were observed. The multiphase of anatase and rutile structure was obtained in comparison with the Joint Committee on Powder Diffraction Standards (JCPDS) Card File No. 21-1272 and 21-1276. The average crystallite size calculated using Scherer's equation for the various peaks were between 246-96.9nm. The XRD pattern of the sol gel deposited $TiO_2$ shows diffraction peaks at 2θ = 25.46, 55.12 43.275 and 63.04. These correspond to three anatase phases; 101 (2θ = 25.46), 211 (2θ= 55.12) and 204 (2θ= 63.04). The peak due to 43.275 and 41.9 could not be identified. It could possibly be due to the FTO substrate. XRD pattern of slot coated $TiO_2$ shows a mixture of anatase and rutile phase structure. Four sharp diffraction peaks of the anatase phase (101, 004, 200, and 204) corresponding to 2θ = 25.3, 37.7, 48.0 and 65.5 respectively, and two sharp peaks of rutile phase (110 and 105) corresponding to 2θ =27.3 and 53.4 respectively, were observed. This is in agreement with literature, [17, 18]. Other peaks are due to the FTO substrate. The average crystallite sizes calculated were between 344-97 nm.

*3.3 Scanning Electron Micrograph (SEM)*

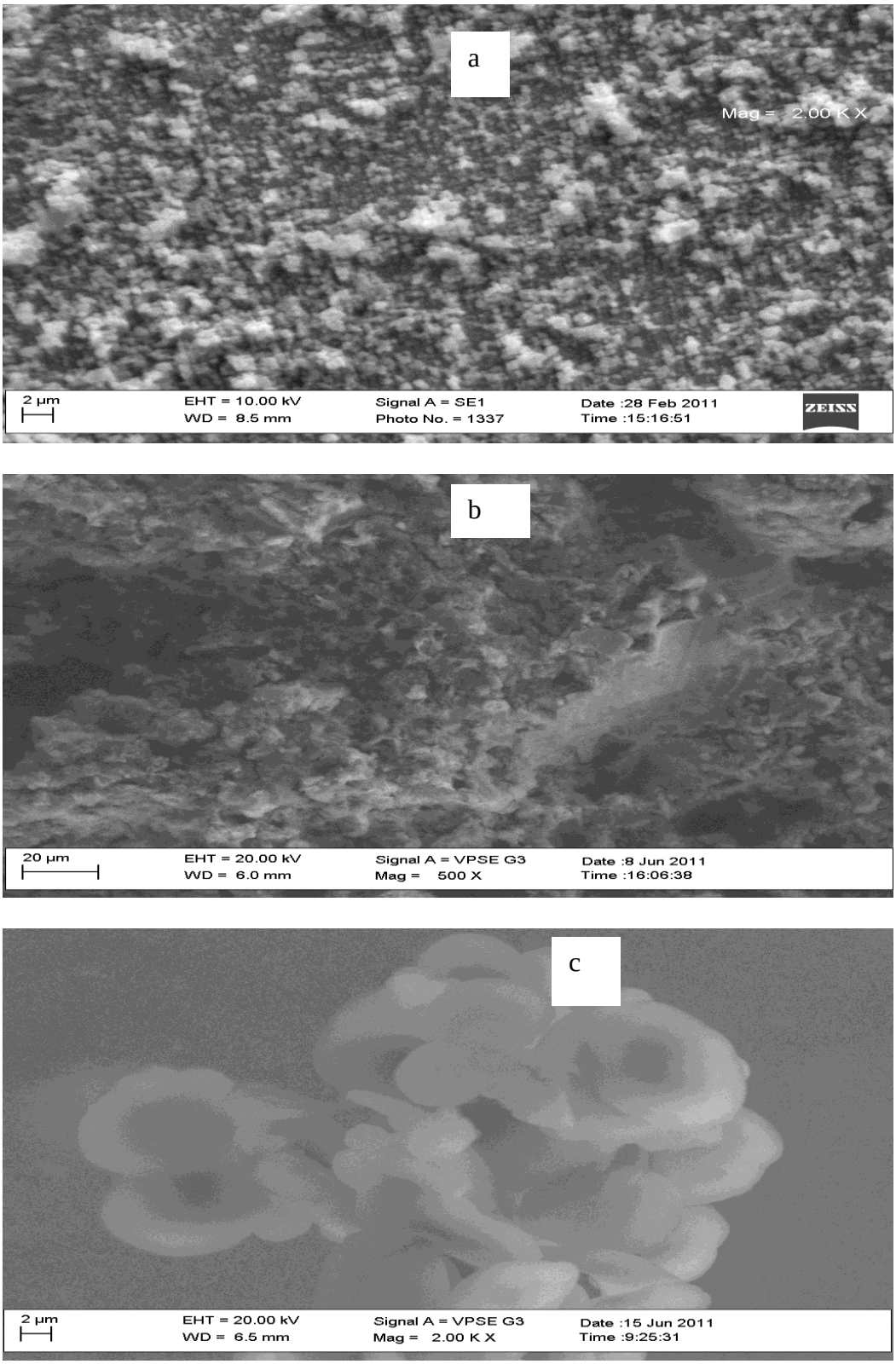


**Figure 4.** SEM image of(a) CBD deposited $TiO_2$ at 2000 magnification (b) sol gel deposited $TiO_2$ at 500magnification (c) slot coated $TiO_2$ at 2000 magnification

The surface morphology of the deposited films was studied using SEM Fig. 4 (a-c) shows the SEM image of CBD, sol gel deposited and slot coated $TiO_2$ respectively. The SEM image of CBD shows that the coating is porous homogenous and closely packed with no gaps between the coatings. The image of the sol–gel deposited $TiO_2$ shows soft and small agglomerates with irregular structure while the image of the slot coated $TiO_2$ shows a smooth coating with a nano-flower-like structure.

### *3.4 Optical Studies*

The optical properties of the films deposited on the FTO substrates were examined for their absorbance and transmittance at normal incident by using a UV-Visible spectrophotometer. The absorbance was measured normally in the wavelength range of 200–1100 nm.

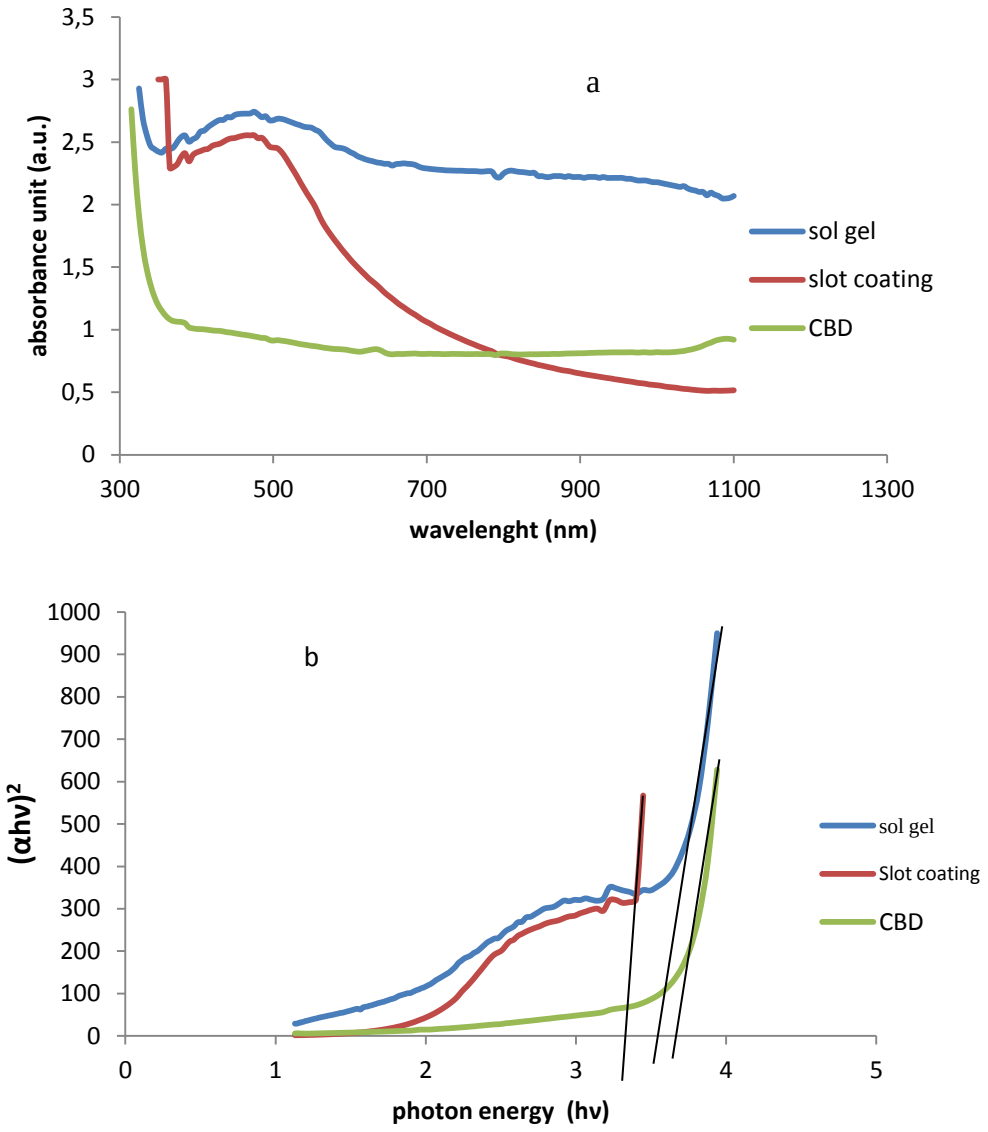


**Figure 5.**(a) Absorbance spectra of the $TiO_2$ films (b) The plot of $(\alpha h\nu)^2$ vs. $(h\nu)$

Band gap was determined by applying Tauc's law. $(\alpha h\nu)^n$ is plotted against (hν) and then the linear part of the curve was extrapolated to $(\alpha h\nu)^n = 0$ [19, 20]. The relationship between the absorption coefficient α and incident photon energy (hν) is written as:

$$(\alpha h\nu)^n = A(h\nu - E_g) \quad 4$$

Where: α is the absorption coefficient, (hν) is the photon energy, A is a constant which does not depend on photon energy, $E_g$ - band gap energy, n is a constant, which depends on the type of transition.

For indirect allowed transition n = ½, while for direct transitions n = 2.

Figures 5a- show the absorbance spectra of $TiO_2$ prepared by the three methods while figure 5b shows a plot of $(\alpha h\nu)^2$ vs. (hν). The absorbance spectra show absorption edges of 385nm for CBD, 370nm for Slot coating and 365nm for Sol gel method. This agrees with what some authors have done and shows that $TiO_2$ absorb in the ultraviolet region and can be used as a UV sensor. Yang et al [21], obtained an absorption edge at 387nm while Sonawane et al [22] obtained an edge at 307nm. The sol gel method and slot coated showed some peak broadening at 485nm and 475nm respectively. These peaks observed in the visible range might not be as a result absorption by $TiO_2$ film but might be as a result of wave interference because $TiO_2$ been a white substance does not absorb in the visible spectrum. None of such peaks was observed for the CBD method. The optical absorption coefficients α were determined from the relative transmission and the sample thickness using equation 5:

$$\text{Absorption coefficient } \alpha = \frac{\ln\left(\frac{1}{T}\right)}{x} \quad 5$$

The obtained values for energy band gaps for $TiO_2$ films determined by plotting $(\alpha h\nu)^2$ vs. (hν) are presented in Table 2 below.

**Table 2.** Values for energy band gap for direct transition

| Sample | Eg determined by applying Tauc's law for direct band gap (eV) |
|---|---|
| CBD | 3.62 |
| Sol gel | 3.53 |
| Slot Coating | 3.22 |

It is seen that the $E_g$ determined gave a value of 3.53 for sol gel, 3.62 for CBD and 3.22 for slot coating. The value for slot coating corresponds to anatase phase of the $TiO_2$. The average literature values for absorption and corresponding band gap energy for bulk anatase $TiO_2$ is λ= 385 nm and

E = 3.2 eV [23-26]. The $E_g$ value obtained for Sol gel and CBD gave a higher value than what was obtained in most publications although Yang et al [21] obtained a value of 3.4 eV for $TiO_2$ deposited on glass substrate while Lei et al [24] obtained a value of 3.5eV for $TiO_2$ sol calcined at 100$^o$C. Mechiakh et al [27] obtained values of 3.7ev and 3.5ev for $TiO_2$ film calcined at 400$^o$C and 450$^o$c respectively. The increase in the optical band gap may be as a result of the grain size being very small.

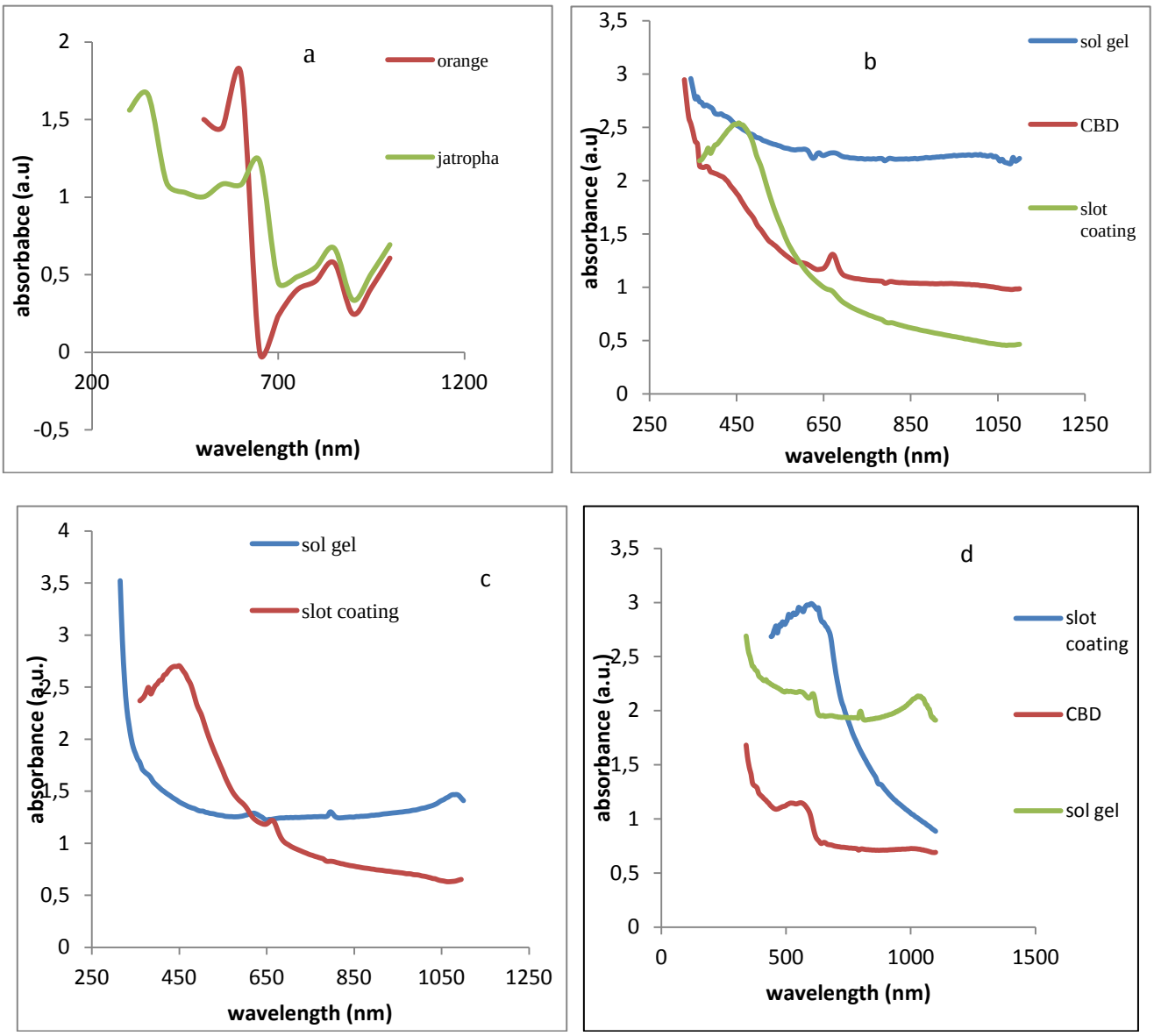


**Figure 6.** (a) Absorbance spectra of Jathropha and Orange extract, (b) $TiO_2$ films stained with Jathropha dye extract, and (c) $TiO_2$ films stained with orange dye extract. (d) $TiO_2$ films stained with R2751 dye

UV-Vis spectroscopy of the extracted natural dyes is shown in figure 6a. Figure 6(b) shows the $TiO_2$ films stained with Jathropha dye extract while fig 6(c) shows $TiO_2$ films stained with orange dye extract. Figure 6(d) shows $TiO_2$ films stained with R2751 dye. It was observed that the orange dye

extract had absorption peaks at 600nm and 850nm corresponding to absorbance values of 1.791and 0.577 respectively while the jathropha dye extract had peaks at 350nm, 650nm and 850nm corresponding to absorbance values of 1.66, 1.231 and 0.671 respectively. These show that the extracts absorbs strongly in the visible region especially in the red region. No blue peak was observed in contrast to what authors who have extracted chlorophyll obtained. Steel et al obtained a blue peak at 425nm and a red peak at 660nm while Gleue [28] obtained a blue peak at 405nm and a red peak at 627nm. Lai et al [29] obtained a blue peak at 430nm and a red peak at 670nm. This shows that different chlorophyll associated with different plants have different spectra. This may be because the pigments are modified by their local protein environment or because the accessory pigments have intrinsically different absorption spectra form [29].

When stained with the jathropha dye extract, the sol gel prepared $TiO_2$ had no observable peak absorption but had higher absorbance value than the other methods over the same wavelength range. The CBD prepared $TiO_2$ stained with the jathropha dye showed peak absorptions at 380nm and 675nm corresponding to absorbance values of 2.263 and 1.294 respectively while the slot coated method had a peak at 465nm at an absorbance value of 2.522.

When stained with the orange dye extract the sol gel method showed small peaks at 615nm and 800nm with absorbance values of 1.267 and 1.218 respectively while the slot coated showed a peak at 445nm corresponding to absorbance of 2.699. In all the stained $TiO_2$, the absorption edge shifted to the visible region showing strong absorption in the visible region.

### *3.5. Current- Voltage (I-V) Characteristics*

A standard solar simulator of light intensity 1000W/$m^2$, spectral distribution AM 1.5 global standard solar spectrum and temperature is 25$^oC$ was used the solar simulation. The sample sizes of the solar cells characterized were typically (1.5x1.5) $cm^2$. Figure 7(a-c) shows the I-V curve in the dark while figure 7 (a-c) shows the illuminated curve of the ruthenium red sensitized cells. The dark I–V curves in the dark indicate good junction rectification properties.

**Table 3.** Summary of the efficiencies of the cell

| | Ruthenium red dye | | | | Jathropha leaf dye extract | | | | Citrus leaf dye extract | | | |
|---|---|---|---|---|---|---|---|---|---|---|---|---|
| | Voc (mv) | Isc (mA) | ff | % | Voc (mv) | Isc (μA) | ff | % | Voc (mv) | Isc (mA) | ff | % |
| Sol gel | 100 | 0.034 | 0.43 | 0.15 | - | - | - | - | 211.5 | 0.011 | 0.71 | 0.16 |
| CBD | 80 | 0.018 | 0.55 | 0.08 | 210 | 0.78 | 0.37 | 0.06 | 180 | 0.026 | 0.21 | 0.01 |
| Slot Coating | 70 | 0.3 | 0.20 | 0.4 | 350 | 65.5 | 0.55 | 1.26 | 310 | 0.114 | 0.30 | 1.06 |

The open circuit voltage, Voc, short circuit current Isc, were determined from the illuminated I-V curves while the fill factor FF and the overall efficiencies η of the solar cells were calculated using equations 6 and 7 respectively. The results are as tabulated below.

$$FF = \frac{V_{PP} .. I_{PP}}{V_{oc} .. I_{sc}} \quad 6$$

$$\eta = \frac{P_{\max}}{P_{light}} = \frac{V_{PP} . I_{PP}}{P_{light}} \quad 7$$

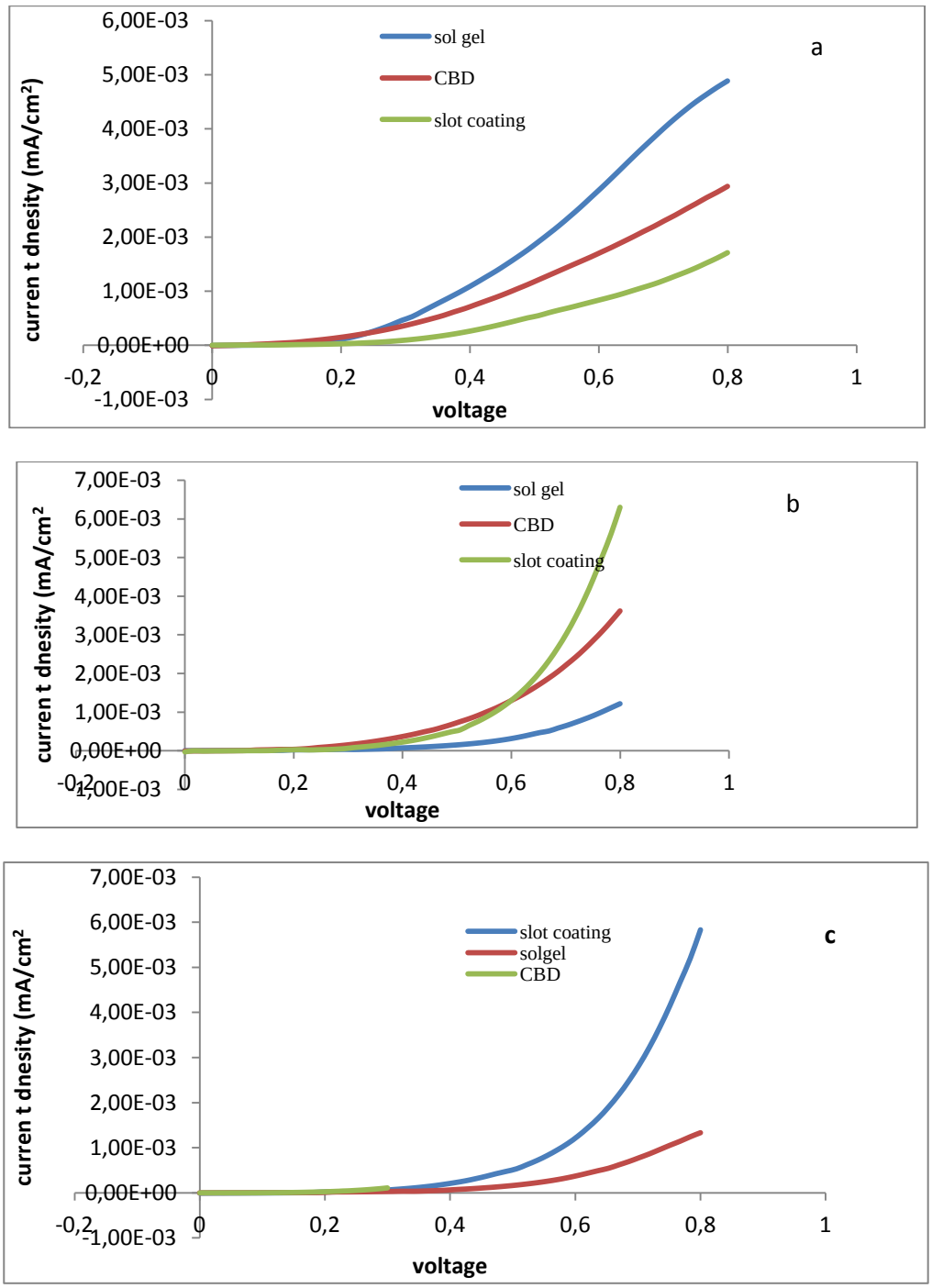


**Figure 7.** I-V curves in the dark for (a) cell sensitized with ruthenium dye (b) jathropha leaf extract, (c) orange leaf extract.

The results show that the the slot coated $TiO_2$ gave the highest efficiency using the the three dyes. With the ruthenium red it gave an efficiency of 0.4% while with jathropha and citrus dye extract an efficiency of 1.26% and 1.06% were obtained respectively. This is comparable with what other authors have obtained. Guterrez-Taste et al [30], obtained an efficiency of 1.8% with N3 ruthenium dye and platinum counter electrode using the commercial Degussa P25 $TiO_2$ powder mixed with water soluble titanium (IV) cis ammonium hydroxide prepared by the slot coating method. Huizhi et al [31] prepared DSSC using Ti-nanoxide paste deposited by the slot coating method with platinum counter electrodes and obtained efficiencies between 0.17-1.17% using various natural dyes and efficiency of 6.11% using N719 dye. Greg and Gratzel [11], obtained efficiencies between 0.5-1.0% using anthocyanin and chlorophyll dye on $TiO_2$ synthesized by the slot coating method. Lai et al [29] prepared DSSC loaded with gold nano particles, sensitized with chlorophyll using P-25$TiO_2$ Degussa powder and obtained an efficiency of 0.705%. Ozuomba et al [32] prepared 1.0% efficient DSSC using chlorin dye extracted from bahama grass on Ti-nanoxide.

The CBD deposited $TiO_2$ gave the lowest efficiency with the three dyes. This may be attributed to the non availability of bonds between the dye and $TiO_2$ molecules through which electrons can transport from the excited dye molecules to the $TiO_2$ film or to the poor adhesion of $TiO_2$ on FTO glass [33]. Similar method used by Zhu et al [34] gave an open-circuit voltage of 0.63 V and a short-circuit current of 7.02 $mA/cm^2$.

The sol gel method gave comparatively better results than the CBD method although the efficiency was still low. The sol gel method with jathropha only gave noise. Liu et al [35], synthesized $TiO_2$ by sol gel process using $TiCl_4$ precursor and obtained an efficiency of 0.99% for the DSSC fabricated with it using platinum counter electrode and N3 ruthenium dye. Jin et al [36] obtained efficiencies in the range of 0.74-1.57% using $TiO_2$ synthesized with titanium (IV) isopropoxide at different concentrations using N719 ruthenium dye.

The low efficiency of the sol gel and the CBD could also be attributed to the use of $TiCl_3$ precursor. The presence of chlorine in the semiconductor could aid in the degradation of the dye, hence affecting the spectral response to the radiation. The quantity of dye adsorbed by each cell could not be ascertained as this also plays a vital role in the amount of radiation absorbed and consequently in the overall efficiency of the cell. Another factor that contributed to the low efficiency of all the cells is the use of carbon counter electrode.

## 4. CONCLUSION

In DSSC $TiO_2$ is the key component in determining the device efficiency. Hence in this study $TiO_2$ was prepared by the slot coating using Degussa P25 powder, the CBD and the Sol gel methods. The chemical, structural, morphological and optical properties of the $TiO_2$ were investigated using Energy Dispersive Spectroscopy EDS, X-ray diffraction XRD, Scanning Electron Microscopy SEM and UV-Visible-Infrared spectroscopy respectively. The chemical composition of all the $TiO_2$ showed the presence of titanium and oxygen in a proportion that indicated the presence of $TiO_2$. The XRD analysis showed a mixture of anatase and rutile phases of $TiO_2$ in both the slot coated and the CBD

deposited films while that of the sol gel was predominantly anatase. The calculated crystallite sizes were in the nanometer range. The morphology of the films showed that they were porous and homogenous. That of the slot coated showed a flower-like structure. The band gap energies determined from the methods were between 3.22-3.62eV. The $TiO_2$ also showed absorption in the ultraviolet spectrum but when coated with the dyes, the absorption shifted to the visible region.

The prepared $TiO_2$ were used to assemble DSSC using red ruthenium dye and dye extracts from jathropha leafs and orange citrus leafs. The electrolyte used was potassium iodine and iodine in acetonitrile solvent and the counter electrode was FTO substrates coated with carbon. The slot coated $TiO_2$ with jathropha leaf dye extract showed the highest overall efficiency of 1.26%. This means that jathropha, apart from its applications in the production of biofuels, the leaves are a good source of natural dye in the fabrication of DSSC.

**References**


1. B. O'Regan M. Grätzel *Nature* 353, (1991) 737.
2. F. Linda., H. Amy, K. Shanks K, P. Bruecken, W. Goates, Institute for Chemical Education Madison, WI (2008).
3. M. Gratzel, JR. Durrant. In Mary D Archer & Arthur J (eds) series on photo conversion of solar energy 3: (2008) 503.
4. M. Gratzel, J of Photochemistry and Photobiology A; *Chemistry* 164 (2004) 1.
5. C. Longo, M. De Paoli, *Journal of the Brazilian Chemical Society* 14, 6, (2003) 889.
6. S. Ito, T.N. Murakami, P. Comte, P. Liska, C. Gratzel, MK. Nazeeruddin, M. Gratzel, *Thin solid Films*, 515, 140, (2008) 4613.
7. G.R.R.A Tennakone, A.R. Kumara, P.M. Kumarasinghe, K.G.U. Sirimanne, J. Wijayantha, *Photochem. Photobiol. A: Chem*., 94, (1996) 217.
8. A. Kay, M. Grätzel, *J. Phys. Chem*., 97, (1993) 6272.
9. S. Hao, J. Wu, Y. Huang, J. Lin, *Sol. Energy*, 80, (2006) 209.
10. D. Zhang, N. Yamamoto, T. Yoshida, H. Minoura, *Trans. Mater. Res. Soc. Japan*, 27 (2002) 811.
11. P.S. Greg, M. Gratzel, *Journal of Chemical Education*, 75, (1998) 752.
12. C.J. Barbe, *Journal of America Ceramic Society*, 80, 12, (1997) 3157.
13. http://www.biofluidtech.com/jatropha.html
14. J. Kowalski, A. Sobczyk-Guzenda, H. Szymanowski, M. Gazicki-Lipman, *Journal of Achievements in Materials and Manufacturing Engineering*, 37/2, (2009) 298.
15. A. Sobczyk-Guzenda**,** M. Gazicki-Lipman**,** H. Szymanowski**,** J**.** Kowalski, P. Wojciechowski**,** T. Halamus, A. Tracz, *Thin film Solids*. 517, 18, (2009) 5409.
16. H. Ninsonti, S. Sangsrichan, W. Kangwansupamonkon, S. Phanichphant, P. Pookmanee, *Journal of Microscopy Society of Thailand*, 23, 1, (2009) 91.
17. A. Karami, *J. Iran. Chem. Soc*., 7, Suppl.9, (2010) S154.
18. D.Guterrez-Taste, Doctoral Thesis submitted to the department de quimica de la Universitat autonoma de Barcelona. (2008).
19. A. Molea V. Popescu, *Optoelectronics And Advanced Materials – Rapid Communications* 5, 3, (2011) 242.
20. R. Zallen M. P. Moret, *Solid communications*, 137, (2006) 154.
21. H. Yang, X. Zhang, Q. Tao, A. Tang, *Journal Of Optoelectronics And Advanced Materials*, 9, 8, (2007) 2493.
22. R.S. Sonawane , S. G. Hegde, M.K. Dongare, *Materials Chemistry and Physics*, 77, (2002) 744.
23. F. Gordillo-Delgado, K. Villa-Gomez, *Superficies y* 24, 1, (2011) 20.

24. G. Lei, X. Mingxia, F. Haibo, *Thin Solid Films*, 515 (2007) 3414.
25. K. Kalyanasundaram, M. Gratzel, *Coordination Chemistry Reviews*, 177 (1998) 347.
26. F. Gordillo-Delgado, K. Villa-Gomez, *Microelectronics Journal* 39, 11, (2008) 1333.
27. R. Mechiakh, B.N. Sedrine. B.J. Naceur, R. Chtourou, *Surface and Coatings Technology*, 206, 2-3, (2011) 243.
28. D.A. Gleue (2011) available at http://teachers.usd497.org/agleue/index.html, assessed 12/07/11
29. W.H. Lai, Y.H. Su, L.G. Toeh, M.N. Hon, *Journal of Photochemistry and Photobiology* A: Chemistry. 195 (2008) 307.
30. D. Guterrez-Taste, I. Zumenta, E. Vigil, X. Domennech, M. A. Hermadez-Fenolosa, A. A. Esteve Jose, *Journal of Photochem and Photobiology A: Chem* 175, (2005) 165.
31. Z. Huizhi, W. Liqiong, G. Yurong, M. Tingli, *Journal of Photochemistry and Photobiology* A: Chemistry. 219 (2011) 188.
32. J.O. Ozuomba, A.J. Ekpunobi, P.I. Ekwo, *Chalcogenide Letters*, 8, 3, (2011) 155.
33. I. Zumeta**,** J.A. Ayllón**,** B**.** González, X. Domenech, E.Vigil, *Solar Energy Materials and Solar Cells*, 93, 10, (2009) 1728.
34. H. Zhu, J. Yang, S. Feng, M. Liu, J. Zhang, G. Li *Applied Physics A: Materials Science and Processing*, (2011) 10.1007/s00339-011-6513-y
35. Y.C Liu, Y.F. Lu, Y.Z. Zeng, C.H. Liao, J.C.Chung, T.Y. Wei, *International Journal of Energy* (2011) Article ID 619069
36. Y.S Jin, K.H. Kim, H.W. Choi, *Journal of the Korean Physical Society*, 57, 4, (2010) 1049